# Lipid bilayer pre-transition as the beginning of the melting process

Karin A. Riske [1,*], Rafael P. Barroso, Cíntia C. Vequi-Suplicy, Renato Germano, Vera B. Henriques, M. Teresa Lamy

*Instituto de Física, Universidade de São Paulo, CP 66318, CEP 05315-970 São Paulo-SP, Brazil*

## ABSTRACT

We investigate the bilayer pre-transition exhibited by some lipids at temperatures below their main phase transition, and which is generally associated to the formation of periodic ripples in the membrane. Experimentally we focus on the anionic lipid dipalmytoylphosphatidylglycerol (DPPG) at different ionic strengths, and on the neutral lipid dipalmytoylphosphatidylcholine (DPPC). From the analysis of differential scanning calorimetry traces of the two lipids we find that both pre- and main transitions are part of the same melting process. Electron spin resonance of spin labels and excitation generalized polarization of Laurdan reveal the coexistence of gel and fluid domains at temperatures between the pre- and main transitions of both lipids, reinforcing the first finding. Also, the melting process of DPPG at low ionic strength is found to be less cooperative than that of DPPC. From the theoretical side, we introduce a statistical model in which a next-nearest-neighbor competing interaction is added to the usual two-state model. For the first time, modulated phases (ordered and disordered lipids periodically aligned) emerge between the gel and fluid phases as a natural consequence of the competition between lipid–lipid interactions.

© 2009 Elsevier B.V. All rights reserved.

## 1. Introduction

The spontaneous self-assembly of lipids into bilayers renders biological membranes their basic lamellar structure. Thus, physico-chemical properties of pure lipid systems have been thoroughly investigated, in order to better understand the structure and features of natural membranes. Special attention has been given to lipid phase transitions, the most well-studied being the gel–fluid transition. This main transition is associated with gauche isomerizations of the acyl chains, which brings the bilayer from an ordered gel to a disordered fluid state. Lipids in biological membranes are mainly in a fluid state, which facilitates lateral mobility and conformational changes of membrane proteins. However, the existence of more ordered domains, such as the so-called rafts, has called the attention to the different membrane packings that might exist in specific regions and could have a biological role [1,2]. Furthermore, some organisms adjust their lipid membrane composition according to the ambient temperature such that their membrane is right above the end of the melting process [3]. Thus, characterization of lipid phases other than the fluid is also biologically relevant.

Some lipids undergo another phase transition below the main one, the so-called pre-transition, in which a flat membrane in the gel phase transforms into a periodically undulated bilayer [4,5]. Although this phase, named ripple phase or $P_{\beta'}$, has been systematically studied, a complete understating of its origin and molecular details is still lacking. Most studies have been performed on phosphatidylcholines (PCs), a major constituent of mammalian cells, which readily form multilamellae with definite interlayer distance when dispersed in water (for a review see [6]). PCs have a fairly bulky headgroup, creating a size mismatch with its acyl chains, especially below the main phase transition. This is believed to be the reason why the acyl chains are tilted in the gel phase of PCs [6,7]. It has been proposed that the driving force for the ripple formation is also coupled to this size mismatch, with headgroup hydration playing an import role [8,9]. It is not yet established whether the chains remain tilted in the ripple phase [10]. Electron density profiles obtained from small angle X-rays scattering (SAXS) of PCs in the ripple phase show an asymmetric undulation pattern resembling a saw-tooth with wavelength of 120–160 Å, depending on chain length [5,10–12]. Studies of the ripple phase are normally done on multi-lamellar systems. Some works propose the existence of surface ripples even in unilamellar vesicles [13,14], although the pre-transition is less cooperative in that case [15]. For multilamellar systems, the rippling of the membrane surface is thought to be coupled to interlamellar distance, thus coherently constructing a lattice that can easily be detected with diffraction techniques. On the other hand, the undulations of single bilayers add incoherently, thus making their detection more difficult [13].

* Corresponding author. Departamento de Biofísica, Universidade Federal de São Paulo, R. Botucatu, 862 7° andar, CEP 04023-062 São Paulo-SP, Brazil. Tel.: +55 11 5576 4530; fax +55 11 5571 5780

E-mail address: kar@biofis.epm.br (K.A. Riske).

[1] Present address: Departamento de Biofísica, Universidade Federal de São Paulo, R. Botucatu, 862 7° andar CEP 04023-062, São Paulo-SP, Brazil.

Generally, it is assumed that the lipids in the ripple phase are mainly in an all-*trans* configuration, as in the gel phase [11]. However, many studies point to the existence of fluid regions coupled with the geometry of the ripples. Sun et al. [10] could model their SAXS data better assuming that the ripples were composed of a long saw-tooth arm, with characteristics of a gel bilayer, and a short arm, thinner and less densely packed, more compatible with a fluid bilayer. Changes of bilayer packing along the undulations were also obtained from molecular [16] and dissipative particle dynamics [17] simulations. Experimental evidence of gel-fluid coexistence in the ripple phase was reported from NMR [18], ESR [19] and SAXS/WAXS [20,21] data. Startlingly, even though so many authors have been stressing for decades the existence of fluid lipids coupled to the ripple geometry, this has not yet become an established knowledge.

Apart from PCs, the pre-transition has been detected also for deprotonated phosphatidylglycerols (PGs) [22–24], although no comprehensive study has been performed with PGs yet. The pre-transition has not been systematically observed for other lipids [8]. The bilayer structure of PCs and charged PGs at 100 mM salt of the same acyl chain was shown to be quite similar [22]. Despite the PG headgroup being considerably smaller than the PC headgroup, its charged character could account for an area per headgroup of the same magnitude. However, this is only true at high ionic strength. At low ionic strength, short chain PGs show peculiar properties and thermal behavior [24–29].

Theoretical studies (see [30] for a general review) in terms of simple statistical models have followed mainly two approaches for explaining the ripple phase: (*i*) *periodic elastic* deformations, mainly due to competition between curvature and tilting of lipids in the *gel* state [9,31–34], although Carlson and Sethna [9] suggested a posteriori that fluid lipids could reside in the packing defects induced by the bilayer corrugation, or (*ii*) *periodic melting* of the chains, which, due to curvature, might imply periodic mechanical undulations [30]. Heimburg [30] was the first to explicitly couple ripple formation with (periodic) chain melting, and to compare experimental DSC data for the pre- and main transitions to results from model simulation. The first group of models [31–34] yield ripple periods dependent on the relation between curvature and tilting parameters, but do not include melting, whereas Heimburg's model [30] requires *ad hoc* introduction of modulation period.

The purpose of this work is to broaden the experimental and theoretical knowledge on the pre-transition and to further explore the idea of the existence of fluid regions coupled to the ripple phase. Experimentally, we compare dispersions of dipalmytoylphosphatidylcholine (DPPC) with its charged analog, dipalmytoylphosphatidylglycerol (DPPG). Because of the net negative charge of DPPG, different concentrations of salt are used. So far, only high ionic strength conditions (at least 100 mM salt) were investigated. Three experimental techniques

are used: differential scanning calorimetry (DSC), electron spin resonance (ESR) of a phospholipid labeled at the end of the hydrocarbon chain (16-PCSL), and the fluorescence of the hydrophobic probe Laurdan, which is also located within lipid bilayers. ESR has been extensively used to monitor the viscosity and polarity of the micro-environment where the nitroxide is localized (see, for example, [35,36]). With the fluorophore Laurdan, the focus is the study of the excitation generalized polarization ($GP_{ex}$) [37], which has been extensively used to detect the coexistence of phases in lipid bilayers [37–39]. We introduce an alternative statistical model, inspired on spin models, which presents modulated phases as an *outcome* of the competing interaction. The main phase transition of lipids is generally well-described using a two-state model [40–43], where interactions between nearest-neighbors give rise to a first order transition between gel (ordered) and fluid (disordered) phases. Based on packing mismatch between heads and tails, we put forward a generalization of this two-state model, where an additional interaction, which favors next-nearest-neighbor pairs in different states, competes with the usual interaction, which prefers adjacent lipids in the same state. The competing interaction yields periodicity. The experimental and simulation results are discussed in terms of the pre-transition being coupled to a periodic lipid melting, associated to the whole acyl chain melting process.

## 2. Materials and methods

### 2.1. Materials

The sodium salt of the phospholipid DPPG (1,2-dipalmitoyl-*sn*-glycero-3-[phospho-rac-(1-glycerol)]), DPPC (1,2-dipalmitoyl-*sn*-glycero-3-phosphatidylcholine) and the spin label 16-PCSL (1-palmitoyl-2-(5-, 14- or 16-doxyl stearoyl)-*sn*-glycero-3-phosphocoline) were purchased from Avanti Polar Lipids (Birmingham, AL, USA). Laurdan (2-dimethylamino-6-lauroylnaphthalene) is from Molecular Probes Inc. (Eugene, OR, USA). The buffer system used was 10 mM Hepes (4-(2-hydroxyethyl)-1-piperizineethanesulfonic acid) adjusted with NaOH to pH 7.4. Mille-Q Plus water (Millipore) was used throughout.

### 2.2. Lipid dispersion preparation

A lipid film was formed from a lipid chloroform solution, dried under a stream of $N_2$ and left under reduced pressure for about 2 h, to remove all traces of the organic solvent. Vesicles were prepared by addition of 10 mM Hepes pH 7.4 with the desired salt concentration, followed by vigorous vortexing above $T_m$. For the ESR measurements 0.2 mol% 16-PCSL and for the fluorescence measurements 0.1 mol% Laurdan was added to the chloroform lipid solution. At this lipid/spin
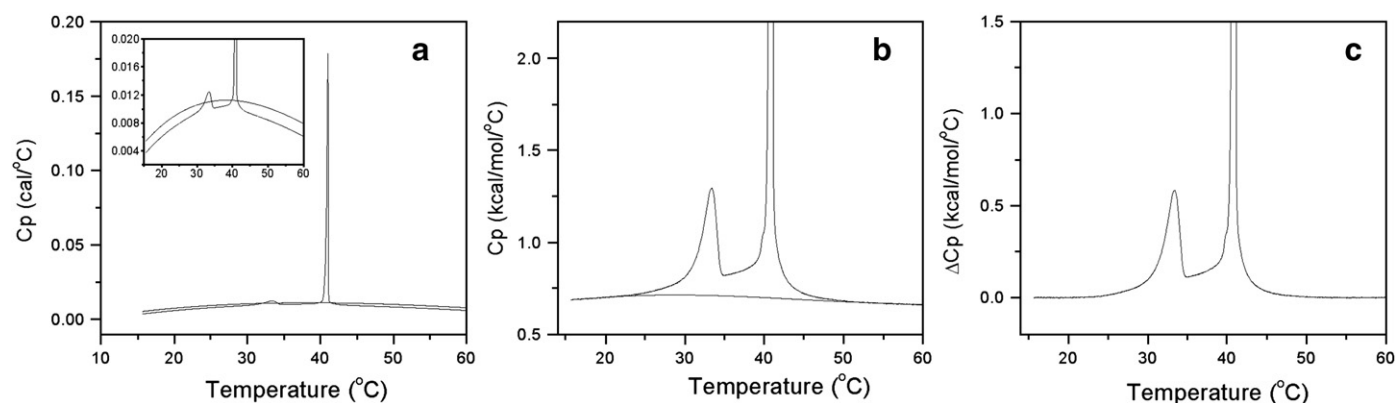


**Fig. 1.** (a) Raw DSC data of 10 mM DPPC and of a buffer-buffer scan. The insert shows a magnification of the data. Scanrate was 10 °C/h (heating). (b) Magnification of the data after subtraction of the buffer–buffer scan and normalization due to the lipid concentration. The line below shows a baseline created manually. (c) Final curve, which is a result of the subtraction of the baseline shown in b).

label ratio no spin exchange linewidth broadening occurred. For the fluorescence measurements, the lipid dispersion was extruded through polycarbonate filters with pores of 100 nm to yield large unilamellar vesicles [44], in order to decrease sample turbidity.

### 2.3. Differential scanning calorimetry

The calorimetric data were carried out in a Microcalorimeter Microcal VP-DSC at a scan rate of 10 °C/h (heating). The thermal profile obtained for DPPC and DPPG at high ionic strength were independent of the scan rate, below 30 °C/h. On the other hand, the profile of DPPG at low ionic strength (with and without 2 mM NaCl) changed slightly with all the scan rates tested (down to 5 °C/h), but within the range of variation found for a series of consecutive scans with the same rate. Fig. 1 shows the sequence of data treatment performed on a typical scan. Data analysis was done using the Microcal Origin software with the additional device for DSC data analysis provided by Microcal: the buffer–buffer scan (shown in Fig. 1a) was subtracted from the raw data, and the resultant curve was then normalized for the lipid concentration (Fig. 1b). Afterwards a baseline was manually created (Fig. 1b) and subtracted, yielding the excess heat capacity $\Delta C_p$ (Fig. 1c). The results shown in Fig. 2 are the final results of the same data treatment done on all curves.

### 2.4. ESR spectroscopy

ESR measurements at X-band (9.4 GHz frequency) were performed with a Bruker EMX spectrometer. Magnetic field modulation amplitude of 1 G and a microwave power of 5 mW were used. The temperature was controlled with a Bruker BVT-2000 variable temperature controller, and monitored with a Fluke 51 K/J thermometer. The ESR spectra of 0.2 mol% 16-PCSL incorporated in DPPC and DPPG were repeated at least twice with samples prepared at different times and the different experiments were compatible. The ESR spectra shown in Figs. 3 and 4 are the best of these experiments. Spectral subtractions were done using the WINEPR software (Bruker).

### 2.5. Fluorescence spectroscopy

The samples were placed in a quartz cuvette, with an optical path of 2 mm. Spectra were measured with a Fluorolog 3 Jobin YvonSPEX, model FL3-11, equipped with a xenon lamp using a 1.5 nm wide bandpass. The excitation spectra were corrected with a quantum counter (Rhodamine B in 3 mg/mL ethylene glycol). Temperature was controlled with a thermal bath Julabo HP 25 and was directly measured in the sample with a digital thermocouple. Excitation spectra were obtained with the emission wavelengths ($\lambda_{em}$) at 440 and 490 nm. From these spectra, the excitation generalized polarization ($GP_{ex}$) as a function of the excitation wavelength ($\lambda_{ex}$) was calculated for each temperature according to [37,45]:

$$GP_{ex}(\lambda_{ex}) = \frac{(I_{440} - I_{490})}{(I_{440} + I_{490})} \tag{1}$$

where $I_{440}$ and $I_{490}$ are the fluorescence intensities at 440 and 490 nm, respectively, at a fixed value of $\lambda_{ex}$. Lipid concentration was 1 mM, to reduce light scattering interferences on the fluorescence measurements. DSC thermal profiles of 1 and 10 mM DPPG and DPPC were found to be very similar. To better analyze the dependence of $GP_{ex}$ with $\lambda_{ex}$, linear fittings were performed, $GP_{ex} = \alpha\lambda_{ex} + b$, and the slopes $\alpha$ plotted.

## 3. Results and discussions

### 3.1. Differential scanning calorimetry

Lipid phase transitions are accompanied by peaks in the heat capacity profile, and can thus be detected with differential scanning
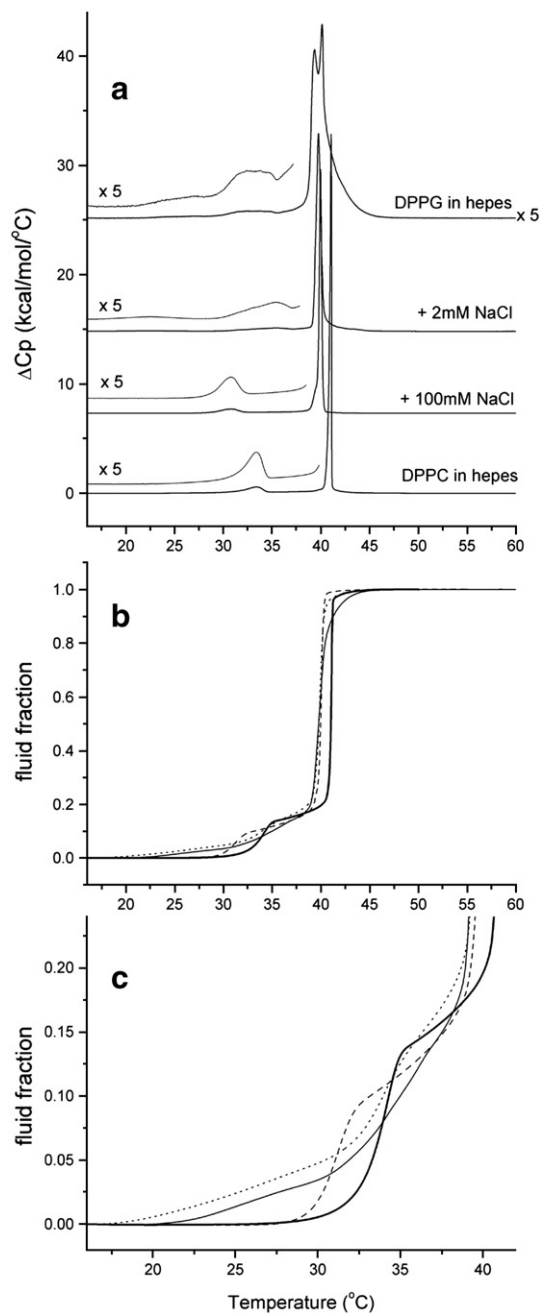


**Fig. 2.** (a) Excess heat capacities ($\Delta C_p$) of 10 mM DPPG in 10 mM Hepes pH 7.4 without and with 2 and 100 mM NaCl, and 10 mM DPPC in 10 mM Hepes pH 7.4. The DPPG in Hepes curve was multiplied by 5. Scans were shifted for clarity. The light curves above each line (below $T_m$) are 5× magnifications of the correspondent curve below. Scanrate was 10 °C/h (heating). (b) Fraction of fluid lipids calculated as the integral of the $\Delta C_p$ curves and normalized by the total enthalpy change $\Delta H$ for DPPG in Hepes (light line), + 2 mM NaCl (dots), + 100 mM NaCl (dashes) and DPPC in Hepes (bold line). Each curve is an average over at least two scans of different samples. The estimated error is around 10% for DPPC and DPPG at high ionic strength and 30% for DPPG at low ionic strength, due to differences among samples. (c) Detail of the pre-transition region of part b).

calorimetry (DSC), which measures the heat capacity at constant pressure as a function of temperature. The lipid main phase transition, also called gel–fluid phase transition, generally gives rise to a very intense and sharp peak of heat capacity. On the other hand, the pre-transition is usually detected as a much less intense and broader peak at lower temperatures. Fig. 2a shows excess heat capacity ($\Delta C_p$) profiles obtained for DPPG, at different concentrations of salt, and for DPPC. PGs and PCs with the same acyl chains are known to exhibit

similar thermal behavior [22]. However, this applies to deprotonated PG in a certain ionic strength range, because of the charge character of its headgroup. Accordingly, dispersions of DPPG in the presence of 100 mM NaCl display a heat capacity profile similar to that of DPPC, as can be seen in Fig. 2a. The very sharp and intense peaks at $T_m = 41$ °C (DPPC) and 40 °C (DPPG in 100 mM NaCl) correspond to the main transition. The broader and less intense peaks at $T_p = 33.5$ °C (DPPC) and 30.8 °C (DPPG in 100 mM NaCl) are related to the pre-transition. For both DPPC and DPPG at high ionic strength, the whole $\Delta C_p$ profile was quite reproducible among different samples, with only minor shifts in $T_m$ and/or $T_p$.

At lower concentration of salt (2 mM NaCl), the main transition of DPPG becomes somewhat broader and the transition temperature shows a minor shift to $T_m = 39.7$ °C. An increase in $T_m$ with the concentration of salt is expected to happen for charged lipids, due to stabilization of the gel phase as a result of headgroup charge screening [46]. The pre-transition is also present for DPPG in 2 mM NaCl, although its $\Delta C_p$ profile is more complex; see Fig. 2a. A maximum in $\Delta C_p$ is detected around $T_p \sim 35$ °C, but the peak is broad and asymmetric. Furthermore, a very broad peak appears at lower temperatures (starting around 20 °C), which might be already connected to the pre-transition. Comparison of thermograms obtained with different preparations (data not shown) shows that the position and profile of the pre-transition peak is sample-dependent, its maximum lying around 32–35 °C. The location of additional lower temperature broad peaks also depends on preparation. On the other hand, the intense $T_m$ peak is very reproducible among different preparations. The thermogram obtained for DPPG in the absence of salt (in Hepes buffer) is even more complex, as even the main transition peak is no longer a single event. The $T_m$ peak splits into two (39.3 and 40.1 °C) and the overall width is larger, as compared to the higher ionic strength condition (note that $\Delta C_p$ is multiplied by five). The exact position and proportion of these two peaks differed to some extent among different samples. This behavior seems to be reminiscent of the complex melting regime of shorter chain PGs, for which an intermediate phase appears between the gel and fluid phases (for a review see [26]). However, the investigation of this possibility is beyond the purpose of the present work. The pre-transition behaves in quite the same way as with 2 mM NaCl: the peak maximum and profile depends on the preparation, its maximum being around 32–35 °C, and lower temperature events start already around 20 °C. Here we have interpreted the broad thermal events starting around 20 °C as the beginning of the pre-transition event, for reasons that will become clearer with the analysis of the fluorescence data, in a following section.

The integral of the excess heat capacity gives the excess enthalpy change $\Delta H$ associated with the transition. The literature values for the enthalpy changes of the pre and the main transition for DPPC and DPPG are around $\Delta H_p = 1$ kcal/mol and $\Delta H_m = 8$ kcal/mol, respectively [15,47]. Our data with DPPC and DPPG agree well with these values. However, the excess heat capacity does not reach the baseline between $T_p$ and $T_m$, being thus difficult to separate both transition events. As mentioned in the introduction, some researchers claim that the melting process starts already at $T_p$, and thus both $\Delta H_p$ and $\Delta H_m$ are parts of one and the same process, namely the melting of the acyl chains [18,21,30]. Our data clearly suggest the same phenomenon, since even for DPPC dispersions $\Delta C_p$ does not level off and continually increases between $T_p$ and $T_m$ (see the magnified curves in Fig. 2a). Following this idea, we can estimate the fraction of fluid lipids as a function of temperature by integrating the excess heat capacity profile and normalizing it by the total enthalpy change, as was first introduced by Hinz and Sturtevant [47], followed by Heimburg [15]. We have calculated this fraction for different samples of DPPC and DPPG in the different concentrations of salt studied, and the average curves for each condition are shown in Fig. 2b. The pre-transition region is shown in detail in Fig. 2c.

The details of the temperature dependence of the fluid fraction of the various conditions studied here are different and sample dependence was observed for DPPG at low ionic strength. However, a general trend can be extracted from our DSC data analysis. A first melting event happens coupled to $T_p$, with associated melting of 5–15% of the lipids, depending on the condition. This event is much cooperative for DPPG at high ionic strength and DPPC and is separated in sequential broad peaks for DPPG at low ionic strength. Between $T_p$ and $T_m$ the fluid population reaches 20% for all conditions. The main transition itself is related to the strong cooperative melting of the remaining 80%. It is interesting to call the attention to this limiting value of 20%, also seen in the data of Heimburg [15]. This might indicate a (geometrical) limiting value for fluid lipids embedded in gel domains.

The pre-transition, and thus the ripple phase, has been generally assumed to be a characteristic of multilamellar structures. However, the fact that the DSC traces of DPPG in 100 mM NaCl and of DPPC are very similar shows that the pre-transition is present also in non-correlated bilayers, as discussed now. From SAXS data [48], DPPG forms unilamellar or uncorrelated lamellae up to 100 mM NaCl. Observation of dispersions of 10 mM DPPG in 100 mM NaCl under an optical microscope revealed the presence of few giant multilamellar vesicles (sizes ~20 μm) coexisting with a leading submicroscopic vesicle population (results not shown). Thus, DPPG in 100 mM NaCl is mostly assembled into submicroscopic vesicles, which might be unilamellar or made of uncorrelated lamellae. Very similar SAXS and optical microscopy results were obtained with DMPG (dimirystoylphosphatidylglycerol) [49].
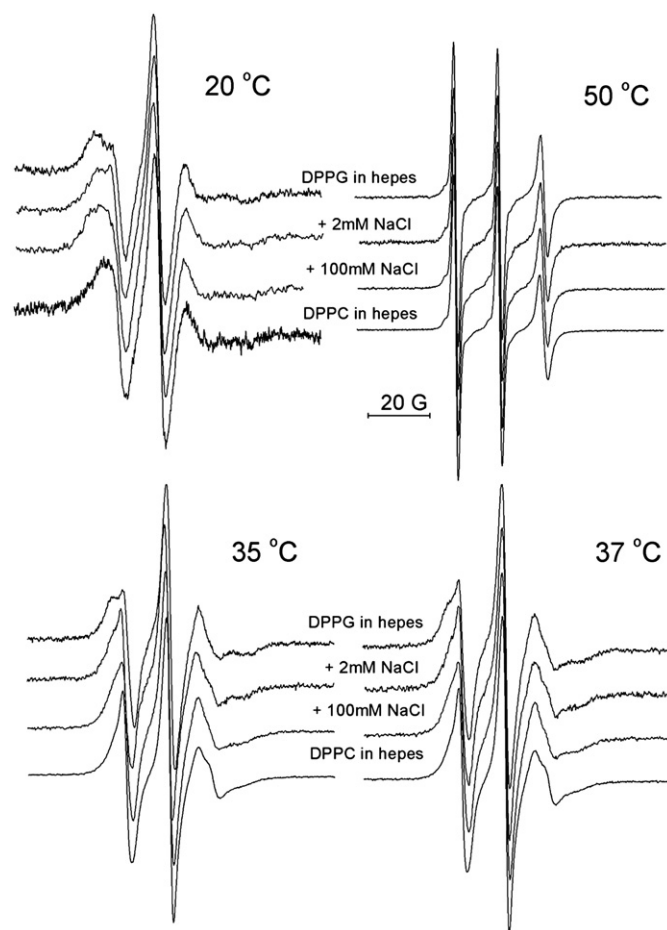


**Fig. 3.** ESR spectra of 0.2 mol% 16-PCSL incorporated in 10 mM DPPC in 10 mM Hepes pH 7.4 and in 10 mM DPPG in 10 mM Hepes pH 7.4 without and with 2 and 100 mM NaCl at 20 °C (below $T_p$), 35 °C and 37 °C (between $T_p$ and $T_m$) and 50 °C (above $T_m$). The spectra were shifted for clarity.

Conversely, only highly dense giant multilamellar vesicles were seen in dispersions of DMPC [49] and DPPC (not shown). We thus conclude that the presence of dominant multilamellar structures is not a pre-requisite for the development of a cooperative pre-transition, since the DSC scans of DPPC and DPPG at high ionic strength are very similar. Thus, the emergence of a ripple phase seems to be dictated by interactions among lipids within a single bilayer. Multilamellae, however, are essential to build up coherence among ripples in different bilayers so that they can be easily detected by diffraction techniques [13].

### 3.2. Electron spin resonance

Electron spin resonance (ESR) of spin labels incorporated in lipid bilayers is a traditional technique to study membrane packing and viscosity [35,36], because it gives information on the mobility, order and polarity of the probe microenvironment. In this work we used a PC lipid labeled with a nitroxide group at the 16$^{th}$ carbon (16-PCSL), thus at the bilayer center. We chose such position because of its high sensitivity to changes in mobility which takes place at the main transition [27]. Probes closer to the headgroup region are partly immobilized even in the fluid phase, because of the reduced degrees of freedom for that position. On the other hand, probes located at the end of the acyl chain experience much more freedom of movement, and changes along the melting process can be better evaluated. Additionally, this probe has proven to be especially adequate for our purpose in previous studies on dispersions of low ionic strength DMPG, which show an extended melting regime. ESR spectra of 16-PCSL were the only ones that could resolve the presence of two distinct populations [27]. If the probe senses two different micro-environments, its spectrum will be a sum of the two populations if the exchange rate between these different locations is slow in the relevant time scale, set by the microwave frequency (nanoseconds). Moreover, in order to detect these two populations in the composite spectrum, differences in their spectral characteristics are necessary. If the exchange rate between the two populations is fast, their differences will be averaged out.

Fig. 3 shows ESR spectra of 0.2 mol% 16-PCSL incorporated in DPPG and DPPC, in the same conditions as studied with DSC, at four different temperatures: 20 °C (below $T_p$), 35 and 37 °C (between $T_p$ and $T_m$) and 50 °C (above $T_m$). In the fluid phase (50 °C) the spectra obtained with DPPC and DPPG with and without salt are all quite similar, with the high degree of motional averaging expected to happen in a fluid phase, inferred from the sharp linewidths and the relatively symmetric heights. On the other hand, the spectra in the gel phase (20 °C) obtained for DPPG and DPPC show a large extent of spectral anisotropy, characteristic of the low mobility and high order of this phase.

The spectra at 35 and 37 °C (Fig. 3), thus between $T_p$ and $T_m$, are those we focus in the present work. If we carefully look at the high field line (first line from the right side), we observe that a second peak is present, being more pronounced in DPPC. In DPPG samples it is only a shoulder, and a second peak can also be identified in the low field line (first line from the left side). Yet, this is a reasonable indication of the presence of two populations, a small amount of a more mobile population, together with a predominant gel phase. It is thus tempting to propose that this corresponds to a small fluid population, consistent with the DSC results.

To test the consistency of this hypothesis, we performed spectra subtractions. Spectra obtained in the fluid phase (40 or 42 °C, depending on the condition) were subtracted from spectra at temperatures between $T_p$ and $T_m$. The percentage of the fluid signal subtracted was varied until the resulting spectrum looked like a one-component signal. Variations on the bilayer packing with temperature in a phase are expected to happen, so the ESR spectrum of a fluid component at 35–37 °C might not be exactly the same as at 40–42 °C. Moreover, lipids located in small fluid regions might experience a slightly different microviscosity than when placed in a complete fluid bilayer. The same reasoning discussed for the fluid phase applies for lipids in the gel phase.

Despite not being able to perform successful subtractions with all spectra between $T_p$ and $T_m$, the features of these spectra suggested the presence of a small percentage of a more mobile component.
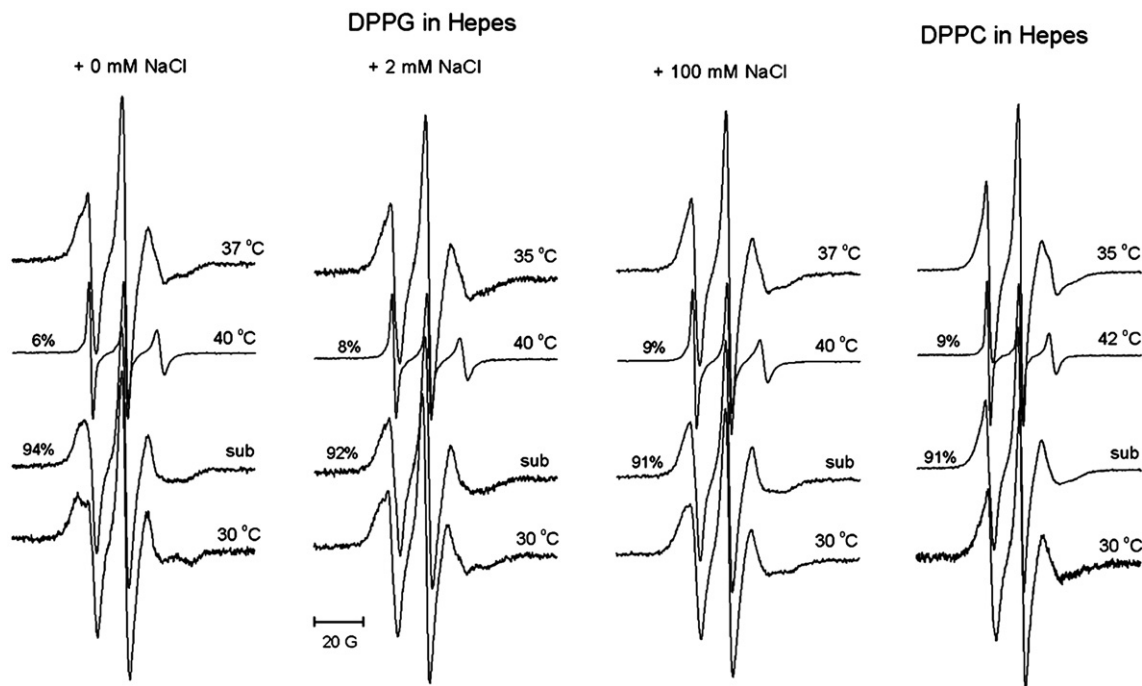


**Fig. 4.** Examples of 16-PCSL ESR spectra subtraction for DPPG at different salt concentrations and DPPC. For each condition, a certain percentage of a spectrum obtained in the fluid phase (marked with 40 or 42 °C) was subtracted from those obtained in the ripple phase (top spectra at the given temperature). The resultant spectra are shown below (indicated by "sub"). The percentage of each component (2nd and 3rd spectra from the top) in the composite spectra (top spectra) is given in the component spectra. The spectra shown at the bottom are experimental spectra obtained at 30 °C, where most of the lipids are in the gel phase.

Examples of reasonable subtractions are shown in Fig. 4. The spectra obtained from the subtractions were similar to spectra at 30 °C for each system (shown for comparison below each subtraction in Fig. 4). As compared to spectra obtained at 20 °C, thus really in the gel phase (see Fig. 3), spectra at 30 °C indicate a somewhat more mobile environment. In fact, for DPPG at all ionic strengths studied, the bilayer is already experiencing the beginning of the melting process at 30 °C (see Fig. 2). From the double integral of the spectrum we can infer the percentage of each population. The fluid component subtracted accounts for 6–9% of the composite spectrum. From the DSC data we have estimated a fluid population around 10–15% at 35–37 °C (Fig. 2c). The subtraction could only be successfully performed when small amounts of the fluid component were present. This is an indication that the microenvironment sensed by the probe in the fluid regions between $T_p$ and $T_m$ is somewhat different than in a complete fluid phase. From the DSC data, lipid melting can start at temperatures as low as 20 °C for DPPG at low ionic strength. The ESR spectra, however, would not be sensitive to the presence of less than ~5% fluid fraction. Evidences for the existence of a fluid fraction could only be detected above 30 °C.

### 3.3. Laurdan fluorescence

The fluorescent probe Laurdan has been widely used to study the gel–fluid transition of lipid bilayers, because it is strongly sensitive to the environment where it resides [39,45,50–52]. Laurdan emission spectra can be decomposed into two bands, with their relative percentages being highly dependent on bilayer packing [52]. The excitation generalized polarization, $GP_{ex}$, measures a normalized intensity ratio between the two emission bands centered around 440 and 490 nm (see Eq. 1 in Material and methods). It has been shown that $GP_{ex}$ is constant for all excitation wavelengths ($\lambda_{ex}$) when Laurdan is incorporated in the gel phase, and steadily decreases with $\lambda_{ex}$ when the bilayer is in the fluid phase. When coexistence of gel and fluid domains is present, $GP_{ex}$ has been shown to linearly increase with $\lambda_{ex}$ [37,45]. To further test the possible gel–fluid coexistence between the pre- and main transitions, Laurdan was incorporated in DPPC and DPPG in Hepes buffer (the lowest ionic strength condition used in the other experiments), and $GP_{ex}$ was calculated from the probe excitation spectrum.

Fig. 5a shows $GP_{ex}$ as a function of $\lambda_{ex}$ for DPPC at four different temperatures: below $T_p$ (20 °C), between $T_p$ and $T_m$ (35 °C), at ~$T_m$ (41 °C), and above $T_m$ (50 °C). Visual inspection of the curves shows that the slopes at 20 and 35 °C are close to zero, at 41 °C the slope is positive and at 50 °C it is negative. However, this does not provide an accurate evaluation of the slopes, although it is the conventional way used in the literature to characterize lipid phases with this probe [38,50,53,54]. To better quantify the slopes of the curves, linear fits were made on the dependence of $GP_{ex}$ on $\lambda_{ex}$ for DPPC and DPPG at all temperatures. As far as we know, this is the first time these slopes are quantitatively analyzed. The angular coefficients $\alpha$ obtained are plotted as a function of temperature in Fig. 5b. The results shown are averaged values obtained from three different experiments. The quantitative analysis of the $GP_{ex}$ slopes reveals the dependence of the Laurdan emission spectrum on $\lambda_{ex}$ with a much better accuracy. Clear and reproducible profiles of $\alpha$ as a function of temperature were obtained for DPPG and DPPC. The careful quantitative analysis of the slopes below $T_m$ reveals that at low temperatures (below ~30 °C for DPPC and ~20 °C for DPPG) $\alpha$ is actually slightly negative, but is roughly independent of temperature (see dashed lines in Fig. 5b). Thus, the gel phase can be characterized by constant slopes, though slightly negative [55]. Between the gel and fluid phases, the slope $\alpha$ increased in two steps. For DPPC, a first small increase happened at 32 °C, coupled to $T_p$, followed by a steady increase up to 37 °C, after which a large increase in $\alpha$ was observed at $T_m$. For DPPG at low ionic strength, $\alpha$ first steadily increased between 20 °C and
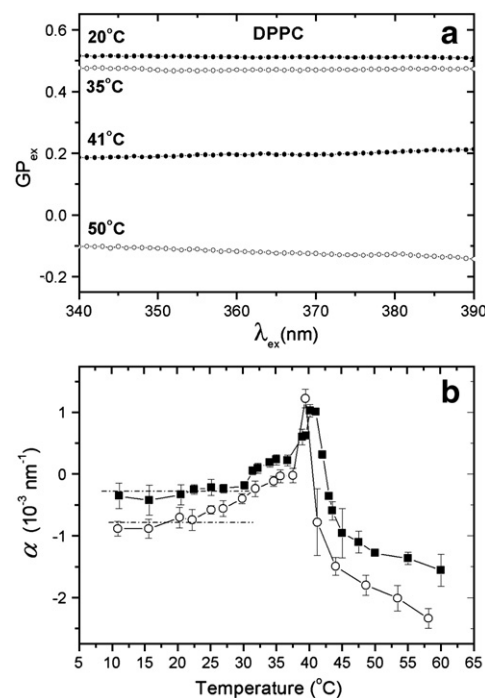


**Fig. 5.** (a) $GP_{ex}$ as function of the excitation wavelength ($\lambda_{ex}$) obtained from the excitation spectra of 0.1 mol% of Laurdan incorporated in 1 mM of DPPC in Hepes buffer, for different temperatures. (b) Temperature dependence of the slope $\alpha$ ($GP_{ex} = \alpha \lambda_{ex} + b$) obtained from linear fits of Laurdan $GP_{ex}$ as a function of $\lambda_{ex}$ in the region between 370 and 390 nm, where clear linear behavior was observed, for DPPG (○) and DPPC (■). The results are the average of three experiments.

37 °C, and then also showed a pronounced increase at $T_m$, when positive values were reached. In the fluid phase (above 42 °C), the linear fits yielded clear negative slopes. Therefore, it is possible to conclude that when $\alpha$ starts to increase from the roughly constant gel phase value, the bilayer is no longer in a homogeneous phase, but contains fluid domains. For DPPC, fluid domains appears in a defined step at $T_p = 32$ °C, whereas for DPPG at low ionic strength, it slowly starts to be perceptible around 20 °C. Laurdan fluorescence was also obtained for DPPG in 2 and 100 mM NaCl, the former resembling DPPG in pure Hepes, whereas the latter showed a similar profile to that observed with DPPC (not shown).

In summary, the dependence of $\alpha$ with temperature extracted from the analysis of the Laurdan spectra parallels that of the fluid fraction obtained from the DSC scans of both DPPC and DPPG (see Fig. 2c). Similar to ESR results, Laurdan fluorescence also indicates gel–fluid coexistence coupled to the ripple phase.

Before proceeding to the statistical model, we would like to make a short summary of the experimental section. The excess heat capacity profile of DPPG at all ionic strengths studied and DPPC (Fig. 2) show that $T_p$ and $T_m$ cannot be completely separated, suggesting that both transitions are related to the same physical phenomenon, namely the acyl chain melting, as proposed earlier [30]. Following this idea, we have estimated that 20% of the lipids melt along the ripple phase, starting with a cooperative event at $T_p$ (Fig. 2c). From ESR spectra subtraction and Laurdan fluorescence (Figs. 3–5) we have confirmed that indeed fluid domains are present in the ripple phase for both lipids. On the other hand, comparing the results obtained for DPPG at different ionic strengths, we conclude that the thermal behavior of DPPG is similar to that of the well-studied DPPC only at high ionic strength (100 mM NaCl). At low ionic strength (0 and 2 mM NaCl), DPPG also displays a pre-transition, but it is less defined/cooperative, sample-dependent, and generally starts at a lower temperature.

## 3.4. Statistical model

The main phase transition has been adequately described by a very simple two-state (gel/fluid) model [31,40–43]. Heimburg [30] was the first to couple the ripple phase to full acyl chain melting. Based on phenomenological arguments, additional interactions between lipids in the two states were considered and a period for the melting "defects" was explicitly included. This new model could simulate two peaks in the excess heat capacity profile. The first smaller peak was associated to the pre-transition and to periodically ordered melting. A second big peak followed at higher temperature, and led to complete melting.

Modulated (periodic) phases have been extensively studied for magnetic spin systems [56–60]. The simpler ferromagnetic phase is described by an analogous two-state model which favors spin alignment. Those studies have led to the discovery that periodic sequences of particles in states of opposite alignment may arise from the addition of a very simple competing interaction with no *ad hoc* periodicity. Modulation comes out as a result from model calculations, but could hardly be predicted a priori, and no qualitative argument which could lead to the prediction of this result exists. Competition between nearest neighbor and next-nearest neighbor interactions along some chosen axis generated modulations of different periods, depending on the competition parameter.

Competing interactions between lipids may also arise from their geometry and hydrophobicity. One of the mechanisms believed to be behind the appearance of the ripple phase is the packing mismatch between a large (hydrated) headgroup and its acyl chains [8,9,61]. Head–tail mismatch may yield a competition, through hydrophobic interactions, between gel and fluid chain states. Consider a row of lipids, as shown in the cartoon of Fig. 6a. Because of head–tail mismatch, a lipid after few gel lipids would be preferentially driven into a fluid state, in order to maintain the integrity of the membrane. This feature can be represented as a favorable interaction between nearest-neighbor lipids in the gel state along with an additional favorable interaction between next-nearest lipids in opposite states.

Note that the packing requirement on head–chain mismatch is satisfied if the line represented in the cartoon is repeated a number of times, giving origin to strips of lipids in the fluid state in the bilayer plane. Thus a competing interaction would be one-dimensional. In analogy to the spin systems, the balance between these two interactions may be expected to create periodic arrays of gel and fluid lipids, under certain conditions.

The presence of fluid lipids embedded in a gel environment would induce kinks on the bilayer surface plane, giving rise to bilayer rippling. The packing frustration within the bilayer discussed here is similar to the picture proposed by Carlson and Sethna [9]. In that paper, however, interactions are treated in terms of elastic energies for tilting of lipids in the gel state. Only a *posteriori*, defects of the gel structure are interpreted in terms of fluid states.

Inspired by the spin models and by this geometric mismatch described above, we propose to analyze the behavior of the two-state (gel/fluid) model with an additional competing interaction, without imposing a specific period. The effective configurational enthalpy may be written in terms of lipid state variables $\eta_i$, which may take values 1 (gel, with degeneracy $D_g$), or 0 (fluid, with degeneracy $D_f$). Using this representation for lipid states, and interactions given in Fig. 6b, we may write an effective enthalpy as

$$H_{eff} = -\varepsilon \sum_{nn} \eta_i \eta_j + \varepsilon K \sum_{nnn} \eta_i \eta_j - \varepsilon R \sum \eta_i \qquad (2)$$

where the first summation in Eq. 2 is over nearest-neighbor ($nn$) pairs, the second over next-nearest-neighbor ($nnn$) pairs along an arbitrary direction and the third one is over lattice sites. Note that the first term favors spatial separation of lipids in the gel from lipids in the fluid state (for $\varepsilon > 0$), whereas the second term favors mixing of lipids in the gel and fluid states, if $K > 0$. The linear term, $R$, dependent on the effective pressure, and on the interaction parameters, favors a pure gel ground state for $R > 0$. The additional competition term may favor special sequences of states along some given direction of the lattice, as is the case for spin models. The direction chosen for the competing interaction is arbitrary and would be defined by some initial nucleation condition.

We have undertaken Monte Carlo [62,63] simulations of the system on a triangular lattice, in the pressure ensemble [64]. Randomly selected lipids are tested for a change of state, according to the Metropolis algorithm, with degeneracy of the gel state accounted for, in order to generate equilibrium Boltzmann distributions at each temperature. We have run our simulations for different lattice sizes $L^2$ and a few sets of parameters for fluid lipid degeneracy and competition, respectively $D = D_f/D_g$ and $K$. Different sequences of calorimetric peaks are found depending on the parameter set chosen. If more than one peak is present, the peaks correspond to the emergence of different modulated phases, followed by complete melting. Also, for different parameter sets the modulated phases display different periods, in accordance with what is known for spin systems [56–60]. On a first exploration of the three-parameter space ($D$, $K$, $R$) we searched for the conditions under which a single modulated phase appeared between the ordered and disordered phases. Data displayed below correspond to a specific set which fulfils such condition. Parameters $D$ and $R$ were taken near the values adopted in studies of the two-state model (in the absence of competition, i.e. $K = 0$) and fittings to experiments [e.g. [40]].

Fig. 7 illustrates our results obtained with $K = 1.2$, $D = 10^4$, $R = 2$ and $L = 10$ for which we have done extensive numerical experiments. Each simulation point corresponds to averages from runs of $10^5$ Monte Carlo steps. In Fig. 7a we show the model specific heat as a function of the reduced temperature ($kT/\varepsilon$), for which two peaks are seen, together with the fraction of lipids in the fluid phase. The first peak is related to partial melting of the chains (around 60%), whereas the second peak is associated to complete disordering of the chains.

The three model parameters, degeneracy $D$, competition interaction $K$ and effective pressure $R$, have different effects on the specific heat profiles. As the degeneracy $D$ is increased, the transitions become sharper, as would be expected. The competition parameter $K$, if sufficiently large, introduces modulated phases between the gel and fluid phases. The modulation period is dependent on the magnitude of $R$, as well as on the other model parameters. At low effective pressures $R$, various transitions, and thus different modulated phases, are present. As $R$ is increased, however, the gel phase is favored, and the modulated phases are gradually suppressed, and at sufficiently high pressure, only the main transition remains. For the same reason, peaks are moved to higher temperatures as pressure increases. Our numerical studies also included variations in the linear lattice size $L$ ($L = 20$, 30, 40 and 80). The results obtained varying the temperature were essentially the same for the same set of parameters, but small bumps appeared in the specific heat peaks for larger lattice sizes.

The presence of modulation was checked by inspection of the correlation function, $g(n)$, for lipids in the gel state. The correlation
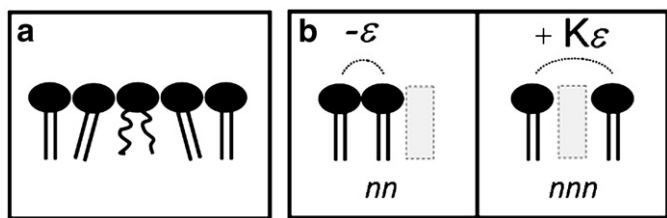


**Fig. 6.** (a) Row of lipids with head–tail packing mismatch. (b) Intermolecular energies considered in the model. Left: attractive nearest-neighbor ($nn$) interactions between a pair of lipids in the gel state. Right: next-nearest-neighbors ($nnn$) interaction along an arbitrarily chosen coordinate axis of the plane.
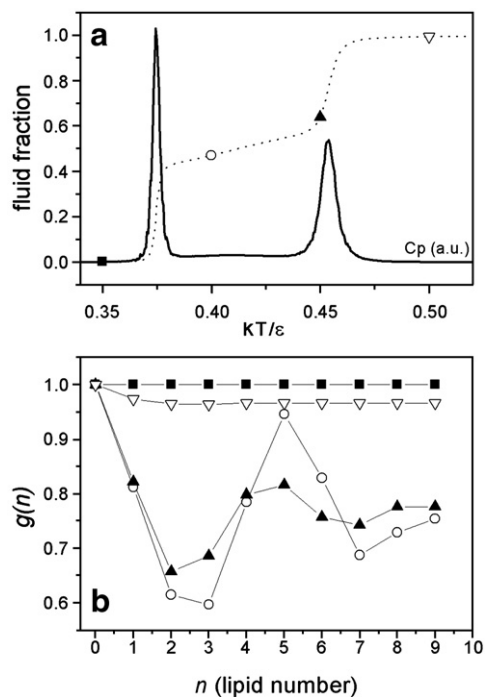
**Fig. 7.** (a) Specific heat (Cp) obtained from the Monte Carlo simulation (solid line) and fluid fraction (dashed line) as a function of the reduced temperature. The points show the temperatures for which the correlation function $g(n)$ was calculated. (b) Correlation function $g(n)$ as a function of the lattice site calculated for four different reduced temperatures: 0.35 (■), 0.40 (○), 0.45 (▲) and 0.50 (▽), shown with the same symbols in a). Parameters used in the Monte Carlo simulations: $K = 1.2$, $D = 10^4$, $R = 2$ and $L = 10$.

function measures the probability of finding a lipid in the gel state at a site position $n$ from a lipid taken as reference. Fig. 7b illustrates the behavior of $g(n)$ measured for temperatures above and below the transition to the modulated phase. Typical configurations are shown in Fig. 8.

The lower temperature peak in specific heat data may thus be associated to partial melting of the chains, as seen from data for fraction of lipids in the fluid state (Fig. 7a). Moreover, data for spatial correlations (Fig. 7b) show that this partial melting is accompanied by the emergence of modulation. Note that the modulation ∼ 3 / 2.5 (gel/fluid) arises naturally from the microscopic model which includes *no* parameter for the modulation.

Comparison of the simulation results (Fig. 7) with those from DSC experiments (Fig. 2) show that agreement is, in this first study, only *qualitative:* we can simulate the emergence of two distinct peaks *coupled* to periodic and global melting of the lipids. However, the *quantitative* agreement is still very poor. The DSC results indicate that the pre-transition accounts for the melting of only 20% of the lipids, whereas model simulations present 60% melting; the DSC pre-transition peak is clearly smaller and broader than the main one, in opposition to the model specific heat; the distance in temperature between the two peaks

obtained from the model is also too large. In its current state the model parameters do not have immediate physical meaning. Thus we could not yet reproduce important features of the experimental profile with our model. Further exploration of parameter space and modulation is under study and shall be the subject of a future work.

## 4. Concluding remarks

In this work we combine experiments and Monte Carlo simulations to broaden the knowledge on the bilayer pre-transition. Experimentally, we have investigated the melting process of DPPG at different concentrations of salt and of DPPC using differential scanning calorimetry, electron spin resonance and fluorescence spectroscopy. Our main experimental finding is that in both lipid systems clear indicatives of up to 20% fluid population were detected between the pre- and the main transitions, in the so-called ripple phase. Thus, our results clearly support the idea that the pre-transition is part of the full acyl chain melting process, as proposed before [30].

Another important result is that at low ionic strength, the pre-transition of the charged lipid DPPG becomes less cooperative, probably indicating a less defined ripple period. We can speculate that headgroup electrostatic repulsion adds an extra interaction that alters the delicate geometrical balance between heads and chains.

We can try to rationalize the data obtained previously with ours. From SAXS data [10,12], typically ∼ 40 lipids build up one ripple period of ∼ 140 Å. If we assume that 10–15% of the lipids melt at $T_p$, as our DSC data suggest (see Fig. 2c), this implies ∼ 4–6 lipids/ripple. These would be enough to stabilize the bilayer kinks. Thus the pre-transition would cooperatively bring the system from a flat to a rippled bilayer, with the fluid lipids geometrically located at the kinks. However, the fluid fraction increases between $T_p$ and $T_m$ reaching 20% (∼ 8 lipids/ripple) just below $T_m$ (Fig. 2c). These melted lipids would be preferentially accommodated in the short arm, as suggested by Sun et al. [10], who showed that this is thinner and less dense than the longer one. Thus a long gel arm seems to coexist with an almost fluid short one just below $T_m$. Further melting of lipids initiates the cooperative transition of the whole system.

We have introduced here a statistical model to further evaluate the interplay between pre-transition and chain melting. Our model combines ideas from the usual two-state model, which describes the gel–fluid transition as a single event [e.g. [40]], and from magnetic spin models, where modulated phases were observed [e.g. [56]]. Based on head–chain packing mismatch, a competition between nearest and next-nearest neighbor interactions among lipids was considered. For a certain set of model parameters, this new model could simulate two calorimetric peaks associated with the melting process. More important, the appearance of gel and fluid lipids in a periodic fashion is a natural consequence of the competition between lipid–lipid interactions. In its current state, the model could qualitatively predict the main experimental observations. A more quantitative description of the melting process using this model is in progress.

The statistical model discussed here does not require multilamellar structures to build up ripples, and is based on packing mismatch on
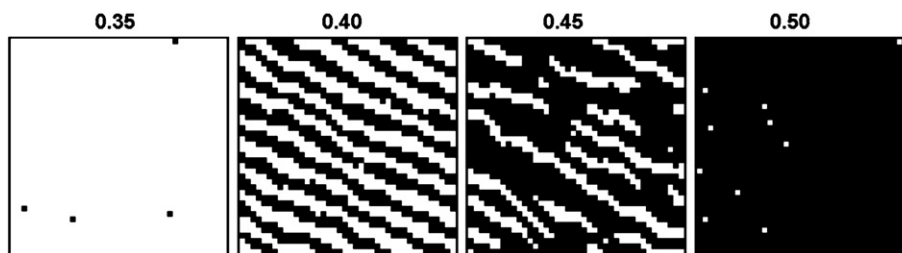


**Fig. 8.** Configurations obtained with Monte Carlo simulation at different reduced temperatures (marked on top; see temperatures in Fig. 7) of gel (white) and fluid (black) lipids. Parameters used in the simulations: $K = 1.2$, $D = 10^4$, $R = 2$ and $L = 40$.

one monolayer. Indeed, as already mentioned, indication of ripples was observed also in unilamellar vesicles [13]. Our experimental data also suggest that a cooperative pre-transition, and ripple formation, can occur on non-correlated bilayers.

The new ideas introduced here may apply to other lipid systems which also have an extended acyl chain melting region. One example is the anionic phospholipid DMPG, for which the gel–fluid transition region extends over more than 10 °C at low ionic strength [26], accompanied by a structural correlation peak around 40 nm [28], which may be related to the emergence of a new type of modulated phase. Generally, the idea of including competition between nearest and next-nearest-neighbor interactions among lipids is new, and might apply to other biologically relevant problems.

## Acknowledgements

## References

[1] D.A. Brown, E. London, Structure and function of sphingolipid- and cholesterol-rich membrane rafts, J. Biol. Chem. 275 (2000) 17221–17224.
[2] K. Simons, E. Ikonen, Functional rafts in cell membranes, Nature 387 (1997) 569–572.
[3] T. Heimburg, A.D. Jackson, On soliton propagation on biomembranes and nerves, Proc. Natl. Acad. Sci. U. S. A. 102 (2005) 9790–9795.
[4] M.J. Janiak, D.M. Small, G.G. Shipley, Nature of the thermal pretransition of synthetic phospholipids: dimyristoyl- and dipalmitoyllecithin, Biochemistry. 15 (1976) 4575–4580.
[5] D.C. Wack, W.W. Webb, Synchrotron X-ray study of the modulated lamellar phase $P_{\beta'}$ in the lecithin–water system, Phys. Rev. A 40 (1989) 2712–2730.
[6] J.F. Nagle, S. Tristram-Nagle, Structure of lipid bilayers, Biochim. Biophys. Acta 1469 (2000) 159–195.
[7] T.J. McIntosh, Differences in hydrocarbon chain tilt between hydrated phosphatidylethanolamine and phosphatidylcholine bilayers. A molecular packing model, Biophys. J. 29 (1980) 237–246.
[8] G. Cevc, Polymorphism of the bilayer membranes in the ordered phase and the molecular origin of the lipid pretransition and rippled lamellae, Biochim. Biophys. Acta 1062 (1991) 59–69.
[9] J.M. Carlson, J.P. Sethna, Theory of the ripple phase in hydrated phospholipid bilayers, Phys. Rev. A. 36 (1987) 3359–3374.
[10] W.-J. Sun, S. Tristram-Nagle, R.M. Suter, J.F. Nagle, Structure of the ripple phase in lecithin bilayers, Proc. Natl. Acad. Sci. U. S. A. 93 (1996) 7008–7012.
[11] K. Sengupta, V.A. Raghunathan, J. Katsaras, Structure of the ripple phase of phospholipid multibilayers, Phys. Rev. E 68 (2003) 031710.
[12] G. Pabst, H. Amenitsch, D.P. Kharakoz, P. Laggner, M. Rappolt, Structure and fluctuations of phosphatidylcholines in the vicinity of the main phase transition, Phys. Rev. E. 70 (2004) 021908.
[13] P.C. Mason, B.D. Gaulin, R.M. Epand, G.D. Wignall, J.S. Lin, Small angle neutron scattering and calorimetric studies of large unilamellar vesicles of the phospholipids phosphatidylcholine, Phys. Rev. E. 59 (1999) 3361–3367.
[14] R.A. Parente, B.R. Lentz, Phase behavior of large unilamellar vesicles composed of synthetic phospholipids, Biochemistry 23 (1986) 2353–2362.
[15] T. Heimburg, Mechanical aspects of membrane thermodynamics. Estimation of the mechanical properties of lipid membranes close to the chain melting transition from calorimetry, Biochim. Biophys. Acta 1415 (1998) 147–162.
[16] A.H. De Vries, S. Yefimov, A.E. Mark, S.J. Marrink, Molecular structure of the lecithin ripple phase, Proc. Natl. Acad. Sci. U. S. A. 105 (2005) 5392–5396.
[17] M. Kranenburg, C. Laforge, B. Smit, Mesoscopic simulations of phase transitions in lipid bilayers, Phys. Chem. Chem. Phys. 6 (2004) 4531–4534.
[18] R.J. Wittebort, C.F. Schmidt, R.G. Griffin, Solid-state carbon-13 nuclear magnetic resonance of the lecithin gel to liquid–crystalline phase transition, Biochemistry 20 (1981) 4223–4228.
[19] D. Marsh, Molecular motions in phospholipid bilayers in the gel phase: long axis rotation, Biochemistry. 19 (1980) 1632–1637.
[20] B.A. Cunningham, A.-D. Brown, D.H. Wolfe, W.P. Williams, A. Brain, Ripple phase formation in phosphatidylcholine: effect of chain relative length, position, and unsaturation, Phys. Rev. E. 58 (1998) 3662–3672.
[21] M. Rappolt, G. Pabst, G. Rapp, M. Kriechbaum, H. Amenitsch, C. Krenn, S. Bernstorff, P. Laggner, New evidence for gel–liquid crystalline phase coexistence in the ripple phase of phosphatidylcholines, Eur. Biophys. J. 29 (2000) 125–133.
[22] A. Watts, K. Harlos, W. Maschke, D. Marsh, Control of the structure and fluidity of phosphatidylglycerol bilayers by pH titration, Biochim. Biophys. Acta 510 (1978) 63–74.
[23] A. Watts, K. Harlos, D. Marsh, Charge-induced tilt in ordered-phase phosphatidylglycerol bilayers evidence from X-ray diffraction, Biochim. Biophys. Acta. 645 (1981) 91–96.

[24] M.F. Schneider, D. Marsh, W. Jahn, B. Kloesgen, T. Heimburg, Network formation of lipid membranes: triggering structural transitions by chain melting, Proc. Natl. Acad. Sci. USA 96 (1999) 14312–14317.
[25] I.S. Salonen, K.K. Eklund, J.A. Virtanen, P.K.J. Kinnunen, Comparison of the effects of NaCl on the thermotropic behaviour of sn-1′ and sn-3′ stereoisomers of 1,2-dimyristoyl-sn-glycero-3-phosphatidylglycerol, Biochim. Biophys. Acta 982 (1989) 205–215.
[26] M.T. Lamy-Freund, K.A. Riske, The peculiar thermo-structural behavior of the anionic lipid DMPG, Chem. Phys. Lipids 122 (2003) 19–32.
[27] K.A. Riske, R.M. Fernandez, O.R. Nascimento, B.L. Bales, M.T. Lamy-Freund, DMPG gel–fluid thermal transition monitored by a phospholipid spin labeled at the acyl chain end, Chem. Phys. Lipids 124 (2003) 69–80.
[28] K.A. Riske, L.Q. Amaral, H.-G. Döbereiner, M.T. Lamy, Mesoscopic structure in the chain-melting regime of anionic phospholipid vesicles: DMPG, Biophys. J. 86 (2004) 3722–3733.
[29] J.-M.I. Alakoskela, P.K.J. Kinnunen, Thermal phase behavior of DMPG: the exclusion of continuous network and dense aggregates, Langmuir 23 (2007) 4203–4213.
[30] T. Heimburg, A model for the lipid pretransition: coupling of ripple formation with chain-melting transition, Biophys. J. 78 (2000) 1154–1165.
[31] S. Doniach, A thermodynamic model for the monoclinic (ripple) phase of hydrated phospholipid bilayers, J. Chem. Phys. 70 (1978) 4587–4596.
[32] M. Marder, H.L. Frisch, J.S. Langer, H.M. McConnell, Theory of the intermediate rippled phase of phospholipid bilayers, Proc. Natl. Acad. Sci. U. S. A. 81 (1984) 6559–6561.
[33] W.S. McCullough, H.L. Scott, Statistical–mechanical theory of the ripple phase of lipid bilayers, Phys, Rev. Lett. 65 (1990) 931–934.
[34] T.C. Lubensky, F.C. MacKintosh, Theory of "Ripple" phases of lipid bilayers, Phys. Rev. Lett. 71 (1993) 1565–1568.
[35] S. Schreier, C.F. Polnaszek, I.C.P. Smith, Spin labels in membranes. Problems in practice, Biochim. Biophys. Acta 515 (1978) 375–436.
[36] D. Marsh, Experimental methods in spin-label spectral analysis, in: L.J. Berliner, J. Reuben (Eds.), Spin Labeling. Theory and Applications, vol. 8, Plenum Press, New York, 1989, pp. 255–303.
[37] T. Parasassi, G. Stasio, G. Ravagnan, R.M. Ruschand, E. Gratton, Quantization of lipids phases in phospholipid vesicles by the generalized polarization of Laurdan fluorescence, Biophys. J. 60 (1991) 179–189.
[38] T. Parasassi, E. Gratton, W.M. Yu, P. Wilson, M. Levi, Two-photon fluorescence microscopy of Laurdan generalized polarization domains in model and natural membranes, Biophys. J. 72 (1997) 2413–2429.
[39] L.A. Bagatolli, E. Gratton, G.D. Fidelio, Water dynamics in glycosphingolipid aggregates studied by LAURDAN fluorescence, Biophys. J. 75 (1998) 331–341.
[40] O.G. Mouritsen, A. Boothroyd, R. Harris, N. Jan, T. Loofman, L. MacDonald, D.A. Pink, Computer simulation of the main gel–fluid phase transition of lipid bilayers, J. Chem. Phys. 79 (1983) 2027–2041.
[41] I.P. Sugár, R.L. Biltonen, N. Mitchard, Monte Carlo simulations of membranes: phase transition of small unilamellar dipalmitoylphosphatidylcholine vesicles, Meth. Enzymol. 240 (1994) 569–593.
[42] I.P. Sugár, T.E. Thompson, R.L. Biltonen, Monte Carlo simulation of two-component bilayers: DMPC/DSPC mixtures, Biophys. J. 76 (1999) 2099–2110.
[43] R. Jerala, P.F.F. Almeida, R.L. Biltonen, Simulation of the gel–fluid transition in a membrane composed of lipids with two connected acyl chains: application of a dimer-move step, Biophys. J. 71 (1996) 609–615.
[44] M.J. Hope, R. Nayar, L.D. Mayer, P.R. Cullis, Reduction of liposome size and preparation of unilamellar vesicles by extrusion techniques, in: G. Gregoriadis (Ed.), 2nd ed., Liposome technology, vol. 1., CRC Press, Boca Raton, FL, 1993, pp. 124–139.
[45] L.A. Bagatolli, T. Parasassi, G.D. Fidelio, E. Gratton, A model for the interaction of 6-Lauroyl-2-(N,N-dimethylamino)naphthalene with lipid environments: implications for spectral properties, Photochemistry and Photobiology 70 (1999) 557–564.
[46] G. Cevc, A. Watts, D. Marsh, Non-electrostatic contribution to the titration of the ordered-fluid phase transition of phosphatidylglycerol bilayers, FEBS Letters 120 (1980) 267–270.
[47] H.-J. Hinz, J.M. Sturtevant, Calorimetric studies of dilute aqueous suspensions of bilayers formed from synthetic L-α-lecithins, J. Biol. Chem. 247 (1972) 6071–6075.
[48] G. Degovics, A. Latal, K. Lohner, X-ray studies on aqueous dispersions of dipalmitoyl phosphatidylglycerol in the presence of salt, J. Appl. Cryst. 33 (2000) 544–547.
[49] R.M. Fernandez, K.A. Riske, L.Q. Amaral, R. Itri, M.T. Lamy, Influence of salt on the structure of DMPG studied by SAXS and optical microscopy, Biochim. Biophys. Acta 1778 (2008) 907–916.
[50] D. Zubiri, A. Domecq, D.L. Bernik, Phase behavior of phosphatidylglycerol bilayers as a function of buffer composition: fluorescence studies using Laurdan probe, Coll. Surf. B: Biointer. 13 (1999) 13–28.
[51] S. Vanounou, D. Pines, E. Pines, A.H. Parola, I. Fishov, Coexistence of domains with distinct order and polarity in fluid bacterial membranes, Photochem. Photobiol. 76 (2002) 1–11.
[52] C.C. De Vequi-Suplicy, C.R. Benatti, M.T. Lamy, Laurdan in fluid bilayers: position and structural sensitivity, J. Fluorescence 16 (2006) 431–439.
[53] S. Palleschi, L. Silvestroni, Laurdan fluorescence spectroscopy reveals a single liquid–crystalline lipid phase and lack of thermotropic phase transitions in the plasma membrane of living human sperm, Biochim. Biophys. Acta 1279 (1996) 197–202.
[54] R.B. Campbell, S.V. Balasubramanian, R.M. Straubinger, Phospholipid–cationic lipid interactions: influences on membrane and vesicle properties, Biochim. Biophys. Acta 1512 (2001) 27–39.
[55] The invariance of Laurdan $GP_{ex}$ with $\lambda_{ex}$ when incorporated in the gel phase of lipids has been justified considering the presence of the probe in a homogeneous

membrane. However, the discussion about the negative values obtained for Laurdan in pure fluid phases are still not clear [37]. We would like to explain the non-zero slopes presented here (Fig. 5b) for lipids in pure gel phase (or fluid phase), which were calculated through a rather accurate methodology, calling attention to the two absorption and emission bands seen in Laurdan spectra [37] in pure phases, which could be attributed to Laurdan in different conformations, absorbing and emitting at different wavelengths (the center of the bands). Hence, it is quite understandable that $GP_{ex}$ would vary with $\lambda_{ex}$, as the relative excitation of the bands would be dependent on the excitation wavelength: the ratio $GP_{ex}$ would be dependent on $\lambda_{ex}$. This discussion is out of the scope of the present work, and will be focused elsewhere (de Vequi-Suplicy, Lamy, Coutinho, in preparation).

[56] W. Selke, The ANNNI model — theoretical analysis and experimental application, Phys. Rep. 170 (1988) 213–264.
[57] N. Bhattacharyya, S. Dasgupta, Statistical mechanics of the 1D ferromagnetic ANNNI chain under an external field: revisited, J. Phys. A: Math. Gen. 24 (1991) 3927–3934.
[58] M.H.R. Tragtenberg, C.S.O. Yokoi, Field behavior of an Ising model with competing interactions on the Bethe lattice, Phys. Rev. E. 52 (1995) 2187–2197.
[59] A. Sato, F. Matsubara, Equilibrium properties of an axial next-nearest-neighbor Ising model in two dimensions, Phys. Rev. B. 60 (1999) 10316–10324.
[60] R.A. Dos Anjos, J.R. Viana, J.R. de Sousa, J.A. Plascak, Three-dimensional Ising model with nearest- and next-nearest-neighbor interactions, Phys. Rev. E. 76 (2007) 022103.
[61] S. Kirchner, G. Cevc, On the origin of the thermal $L_{\beta'} \rightarrow P_{\beta'}$ pretransition in the lamellar phospholipid membranes, Europhys. Lett. 28 (1994) 31–36.
[62] M.E.J. Newman, G.T. Barkema, Monte Carlo Methods in Statistical Physics, Clarendon Press, Gloucestershire, 1999.
[63] D.P. Landau, K. Binder, A Guide to Monte Carlo Simulations in Statistical Physics, 2nd ed.Cambridge University Press, Cambridge, 2005.
[64] H.B. Callen, Thermodynamics and an Introduction to Thermostatistics, 2nd ed. John Wiley & Sons Inc., Singapore, 1985.